A Novel Hybrid Home Energy Management System Considering Electricity Cost and Greenhouse Gas Emissions Minimization

Sara Barja-Martinez, Fabian Rücker, Mònica Aragüés-Peñalba, Roberto Villafafila-Robles, Íngrid Munné-Collado, and Pau Lloret-Gallego

***Abstract*—This article proposes a multiobjective hybrid energy management system that minimizes both the electricity expenses and the household greenhouse gas emissions released due to consumption, considering the entire life cycle of the generation assets used to provide energy. The global warming potential indicator is used to decide if it is more sustainable to purchase electricity from the grid or use the household's flexible generation sources like photovoltaic panels and the energy storage system. Results prove that it is possible to reduce greenhouse gas emissions without incurring expensive electricity bill costs thanks to the hybrid-based home energy management system approach. This method gives the end-users a more influential role in the climate change solution, allowing them to give more or less importance to the economic or environmental component, according to their preferences.**

***Index Terms*—Batteries, flexibility, greenhouse effect, life cycle assessment, multiobjective optimization.**

I. Introduction

GLOBAL carbon dioxide emissions reached in 2019 an all-time high, despite coal fading [1]. Decarbonization is vital; for this reason, the electricity sector has already started moving from fossil-based to net-zero greenhouse gas (GHG) emissions thanks to the increasing number of renewable energy sources (RES) and the use of flexibility in the power system to enhance the grid integration and maximize renewable energies potential. A long-term forecasting study about the evolution of the global energy transition is conducted in [2]. Key findings predict a sharp drop in fossil-fuel use (around 75% by 2050) and warn that the Paris agreement will not be accomplished if no further decarbonization measures are taken. Focusing on Europe, current policies will reduce GHG emissions by 60% in 2050 compared to 1990 emissions levels. Nevertheless, the European Commission has increased its climate ambition through the European Green Deal by enumerating key transformative economic policies and measures to put Europe on track to achieve the goal of net-zero global warming emissions by 2050.

Concerning the residential sector, buildings and households play a crucial role in the energy transition. In 2018, they represented 28% of the global energy-related carbon dioxide emissions [1]. Due to the still existing margin of improvement in the energy efficiency field, buildings are expected to be the fastest sector reducing the CO_2 emissions [3]. Thus, more robust strategy measures to decrease GHG emissions associated with residential electricity demand need to be addressed.

This article proposes that intelligent home energy management systems (HEMS) contribute to achieve environmental targets. In literature, there are principally two HEMS approaches: price based (PB)—most of the current work—and incentive based (IB). The PB program aims to minimize the end-user electricity bill by rescheduling controllable flexible sources optimally, considering a dynamic pricing tariff. Several studies have applied multiobjective functions HEMS for optimal scheduling considering electricity cost and end-user discomfort minimization [4]–[12]. For instance, Di Piazza *et al.* [8] minimized electricity cost and the power profile deviation at the point of common coupling, while Huang *et al.* [9] proposed a cost-effective HEMS considering thermal and electricity comfort. The IB program offers flexibility to a third electricity agent to exchange economic compensation for changing its baseline consumption. Sattarpour *et al.* [13] assured minimum energy cost and supports the upstream micro-grid operation by minimizing the load profile deviation. Electric vehicle and electric water heater provide flexibility in [14] for PB and IB programs. A third environmental-based (EB) category has been proposed in [15], which focuses on minimizing the GHG emissions produced by the generation units that provide electricity to the household. The study carried out in [16] presents a multiobjective dispatching optimization model of an energy system focused on the energy production, conversion, and storage to maximize

Manuscript received October 13, 2020; revised December 23, 2020; accepted January 30, 2021. Date of publication February 3, 2021; date of current version May 19, 2021. Paper 2020-SECSC-1534.R1, presented at the IEEE International Conference on Environment and Electrical Engineering and the IEEE Industrial and Commercial Power Systems Europe, Madrid, Spain, Jun. 9–14, 2020, and approved for publication in the IEEE Transactions On Industry Applications by the Renewable and Sustainable Energy Conversion Systems Committee of the IEEE Industry Applications Society. This work was supported by the Ministerio de Ciencia, Innovación y Universidades under Grant RTI2018-099540. The work of Sara Barja-Martinez and Íngrid Munné-Collado was supported by the Generalitat de Catalunya under the FI-AGAUR Predoctoral grants and scholarships, and has been cofunded by the European Social Fund. The work of Mònica Aragüés-Peñalba was supported by the Department of Electrical Engineering, UPC of the Serra Húnter programme. *(Corresponding author: Sara Barja-Martinez.)*

The authors are with the Department of Electrical Engineering, CITCEA-Universitat Politècnica de Catalunya, 08028 Barcelona, Spain (e-mail: sara.barja@upc.edu; fabian.rucker@upc.edu; monica.aragues@citcea.upc.edu; roberto.villafafila@upc.edu; ingrid.munne@upc.edu; pau.lloret@upc.edu).

Color versions of one or more figures in this article are available at https://doi.org/10.1109/TIA.2021.3057014.

Digital Object Identifier 10.1109/TIA.2021.3057014

TABLE I
HEMS PROGRAMS AND THEIR SERVICES

HEMS program	Description	HEMS service
PB [4]–[7], [13], [14], [18]–[20]	The objective is to minimize the end-users electricity bill.	Time-of-use pricing, real-time pricing and peak shaving.
IB [13], [14], [21], [22]	Flexible sources are economically incentivized to be flexible by modifying their electricity use.	Providing flexibility to a third energy agent.
EB [15]	Flexibility is used to minimize the GHG emissions of buildings associated to generators that produce the electricity they consume.	Minimization of GHG.

TABLE II
LYFE CYCLE EMISSION FACTORS FOR ELECTRICITY GENERATION SOURCES

Generation source GS_i	GWP range [kg CO_{2-eq}/kWh]	Average GWP [kg CO_{2-eq}/kWh]
Hard coal	0.66-1.05	0.855
Lignite	0.8-1.3	1.050
Natural gas	0.38-1	0.69
Nuclear	0.003-0.035	0.019
Biomass	0.0085-0.13	0.0693
Hydro-power	0.002-0.02	0.011
Photo-voltaic	0.013-0.19	0.1015
Wind	0.003-0.041	0.022
Battery	-	0.0706

Extracted from [23].

the operating revenue and to minimize operational risk and carbon emissions. Focusing on HEMS sustainability factors, the study [17] calculates climate effects by displaying carbon emissions at customers' premises to motivate them to diminish their consumption. In [18], curtailment of on-site PV is penalized to maximize green energy consumption.

This article introduces a hybrid-based (HB) HEMS, which is a mixture of the already mentioned PB and EB approaches. Some HEMS programs found in literature are listed in Table I. The vast majority of the studies focus on PB programs, which is also stated by [14]. Some works propose multiobjective functions that consider both PB and IB programs [13], [14], [16].

To the best of the authors knowledge, no HEMS approach in literature focuses on both electricity bill and GHG minimization. The most significant contributions of this article are summarized as follows.

1) The development of a multiobjective hybrid HEMS that minimizes the costs and the GHG emissions associated with generators that produce the electricity that the household consumes by assigning weights to the two competing objectives.
2) The implementation of a life cycle assessment (LCA) methodology to measure the impact that each generation technology has on the climate, from cradle-to-grave. Thus, all the emissions expected during its life cycle are considered, having a more realistic picture of the emissions released into the atmosphere.
3) The implementation of a degradation battery model focused on HEMS that considers calendar and cycling aging constraints.
4) The proposed HEMS enables the end-users to have a more influential role in the climate change solution by giving more weight to the multiobjective function's environmental component.

The following bullets enumerate the research gaps.

1) Controllable flexible electrical loads are not considered in this article.
2) Due to the previous point, the discomfort penalization is not in the HEMS objective function since the only flexible sources are battery and PV generator.
3) The case studies proposed are two extreme opposing energy mix scenarios, one with 83.07% of noncarbon emissions generation share, and the other with 29.18%. The intention is to highlight the HB HEMS potential.

This article is structured as follows. The LCA methodology and the time-varying global warming potential indicator of the generation technologies are explained in Section II. The mathematical formulation is expressed in Section III. Section IV explains the case studies for evaluating the three HEMS proposed, while the results and sensitivity analysis are presented and discussed in Section V. Finally, Section VI concludes this article.

This article is an extension of previous study conducted by the authors [15].

II. LCA FOR ELECTRICITY GENERATION SYSTEMS: A TIME-VARYING GWP APPROACH

This section estimates the real environmental impact considering the entire life cycle of an electricity generation system, using the LCA methodology whose evaluation goes from raw materials and fuel extraction to the gate of the generation plant, through materials processing, plant operation and maintenance, and plant infrastructure commissioning and decommissioning. Global warming potential (GWP) is the LCA impact category selected as the reference measure to quantify and assess the potential environmental impact of an electricity generation source. The GWP indicators for the electricity generation sources evaluated in this article are noted in Table II and were obtained from [23].

Power systems consisting of diverse generation sources have time-dependent GHG emissions; therefore, the GWP performance changes over time along with the electricity mix [24]. One of the objectives is to calculate the hourly kg CO_2 equivalent (CO_{2-eq}) in one kWh of the energy mix. The hourly average GWP impact of the electricity supply from the grid is expressed as

$$\mathrm{GWP}_t^{\mathrm{grid}} = \sum_{i \in I} \mathrm{GWP}_i^{\mathrm{avg}} \cdot \mathrm{GS}_{t,i} \tag{1}$$

where $\mathrm{GWP}_i^{\mathrm{avg}}$ is the GWP average constant for each type of generation source i and $\mathrm{GS}_{t,i}$ refers to the estimated generation in the day-ahead market at period t for each type of generation source i. Table II shows the GWP indicator range for the overall life cycle stages for each electricity generation source type, according to [23]. This article applies the average GWP value.

III. Mathematical Formulation

This section covers the three HEMS objective functions approaches -PB, EB, and HB- and mathematical formulation of the optimization model for controlling and rescheduling flexible household sources.

A. HEMS Objective Function

1) Price-Based Program: This program focuses exclusively on the economic aspect. It aims to minimize the electricity bill (2a), considering the battery degradation cost K_t^{calendar} due to calendar aging, where P_t^{buy} is the time-varying electricity price, χ_t^{buy} refers to the energy purchased to the grid, and P^{VAT} is the tax applied. Constraint (2d) ensures that the energy balance is always met, where ψ_t^{pv} is the optimized PV generation output and W_t^{inflex} stands for inflexible household consumption. Finally, constraint (2d) avoids exceeding the contracted power $X^{\text{max,imp}}$. To switch from power to energy units, N^{hour} is used, which refers to the number of periods per hour. The objective function is expressed as

$$\min_{\chi,V} z_1 = \sum_{t\in T}(P_t^{\text{buy}}\chi_t^{\text{buy}}P^{\text{VAT}} + K_t^{\text{calendar}}) \tag{2a}$$

$$K_t^{\text{calendar}} = 0.019 \cdot V_t - 0.0629 \tag{2b}$$

$$\psi_t^{\text{pv}} + \sigma_t^{\text{dis}} + \chi_t^{\text{buy}} = \sigma_t^{ch} + W_t^{\text{inflex}} \tag{2c}$$

$$\chi_t^{\text{buy}} \le X^{\text{max,imp}}/N^{\text{hour}} \tag{2d}$$

2) Environmental-Based Program: This program attempts to minimize the carbon footprint occasioned by the generation sources that provide electricity to the household. This HEMS is presented in [15]. The objective function is formulated as follows:

$$\min_{\chi,\psi,\sigma} z_2 = \sum_{t\in T} \text{GWP}_t^{\text{grid}}\chi_t^{\text{buy}} + \text{GWP}^{\text{pv}}\psi_t^{\text{pv}} + \tag{3a}$$

$$+ \text{GWP}^{\text{bat}}\sigma_t^{\text{dis}} \tag{3b}$$

s.t.

$$\psi_t^{\text{pv}} + \sigma_t^{\text{dis}} + \chi_t^{\text{buy}} = \sigma_t^{ch} + W_t^{\text{inflex}} \tag{3c}$$

$$\chi_t^{\text{buy}} \le X^{\text{max,imp}}/N^{\text{hour}} \tag{3d}$$

where $\text{GWP}_t^{\text{grid}}$ indicates the kg CO_{2-eq}/kWh of the grid on average per period t. It is calculated with the hourly energy production mix, taking the values of scheduled generation in the day-ahead market for each technology described in Table II.

3) Hybrid-Based Program: This approach is a multiobjective problem (MOP) that combines the PB and the EB objective functions. It is a multiple criteria decision-making problem with no unique optimal solution, but a domain of feasible solutions that satisfy all constraints. Therefore, the result is a tradeoff, a compromise between minimizing the energy costs and decreasing GHG emissions derived from the generation sources that provide electricity to the house.

The HB objective function z_3 is formulated in (4a). Normalization of the objectives is required so that both competing objectives can be equivalent and compared at the same level. z_1^* is the optimal solution of the PB objective function z_1 (2a), and z_2^* is the optimal solution of the EB objective function z_2 (3b). The linear MOP is formulated as

TABLE III
HEMS Programs' Objective Functions

Objective function	Mathematical formulation
Price-based	$[MIN]z_1 = \sum_{t\in T}(P_t^{buy}\chi_t^{buy}P^{VAT} + K_t^{calendar})$
Environmental-based	$[MIN]z_2 = \sum_{t\in T}(GWP_t^{grid}\chi_t^{buy} + GWP^{pv}\psi_t^{pv} + GWP^{bat}\sigma_t^{dis})$
Hybrid-based	$[MIN]z_3 = \frac{\alpha z_1}{z_1^*} + \frac{\beta_2}{z_2^*}$

$$\min_{\chi,\psi,\sigma,V} z_3 = \frac{\alpha \cdot z_1}{z_1^*} + \frac{\beta \cdot z_2}{z_2^*} \tag{4a}$$

$$K_t^{\text{calendar}} = 0.019 \cdot V_t - 0.0629 \tag{4b}$$

$$\psi_t^{\text{pv}} + \sigma_t^{\text{dis}} + \chi_t^{\text{buy}} = \sigma_t^{ch} + W_t^{\text{inflex}} \tag{4c}$$

$$\chi_t^{\text{buy}} \le X^{\text{max,imp}}/N^{\text{hour}} \tag{4d}$$

$$\alpha + \beta = 1 \tag{4e}$$

where α and β are weighting factors for PB and EB objective function, respectively. The sum of these two factors must be one (4e). To conclude, Table III shows the formulation of the objective functions of the three HEMS programs.

B. Energy Storage System

Battery aging is formed by calendar and cycling aging. Calendar aging happens during the battery rest time, whereas cycling aging is caused directly by charges and discharges. According to [25], the Li-ion battery degradation due to cycling shows minimal aging for low current rates [26] and also when the battery is not charged to its real maximum state of charge (SOC) since there is a faster degradation when charging to 100% SOC. Therefore, the following constraints explained in Section III-B2 are added to the battery model to ensure that the storage unit works under conditions that minimize the cycle aging impact.

1) Equation (13) ensures that the battery charges and discharges at low current rates.
2) Equation (14) reduces large cycles at high SOC by limiting the maximum SOC allowed.

Given the above, the battery calendar aging is formulated.

1) Battery Calendar Aging: Battery operating conditions have a significant impact on their performance and life time. The storage model applied in this article considers calendar aging for a lithium-ion (Li-Ion) battery. This phenomenon leads to a decrease in usable battery capacity and an increase in the battery's inner resistance over time, resulting in a depreciation cost. The calendar aging model formulation applied in this article is parametrized in [26] through accelerated aging tests. The capacity defined in (5) is a phenomenon, where the volume of energy that a battery can operate at the rated voltage diminishes over time [27]. The variables that impact calendar aging, thus influence battery life time, are cell temperature and voltage. The loss of capacity is more prominent than the resistance increase in the calendar aging function according to [26], as the end of

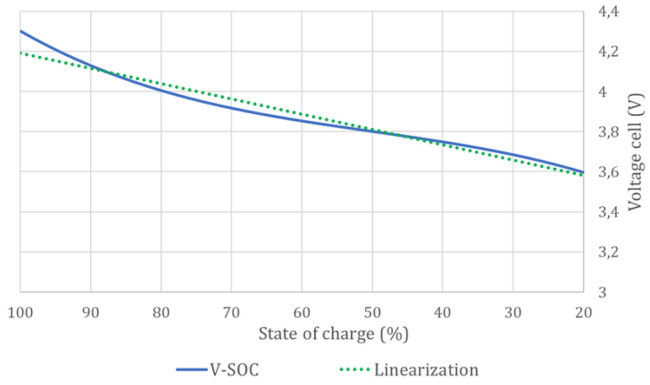

Fig. 1. Linear and nonlinear OCV and SOC dependence.

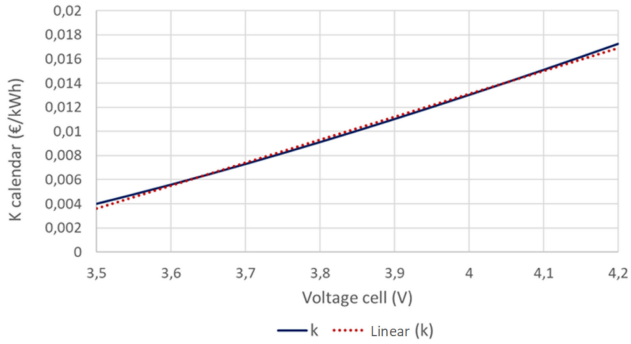

Fig. 2. Dependence of cell voltage on SOC for a cell temperature of 293 K and time step $\Delta t = 15$ min.

the battery life is reached first due to the loss of capacity. For this reason, only the capacity is considered in the calendar aging formulation.

For a Li-Ion battery cell, the capacity C due to calendar aging is expressed as

$$C(t) = 1 - \psi(V,T) \cdot t^{0.75} \tag{5}$$

where ψ is an aging factor that describes the aging rate during period t and is formulated as

$$\psi(V,T) = (a \cdot V_t^{\text{cell}} - b) \cdot e^{-c/T} \tag{6}$$

where temperature is a constant parameter $T = 293\ K$ in this article, $a = 7.543 \cdot 10^6\ V^{-1}\text{days}^{-0.75}$, $b = 2.375 \cdot 10^7\ \text{days}^{-0.75}$, and $c = 6976\ K$ [26].

The relationship between the open-circuit voltage (OCV) and SOC is known and expressed by the nonlinear equation shown in Fig. 1. In order to avoid nonlinear constraints, the dependence between the OCV of the cell and SOC is linearized. The minimum SOC by restriction is limited to 25%.

As a result, the linear correlation is represented as

$$V_t^{\text{cell}} = 0.0076 \cdot SOC_t + 3.4287 \tag{7}$$

where variable SOC_t indicates the percentage of energy stored per period t. The depreciation of the battery during each time step Δt leads to K_t^{calendar} costs

$$K_t^{\text{calendar}}(L, \Delta t) = \frac{K^{\text{investment}}}{L} \Delta t \tag{8}$$

where $K^{\text{investment}}$ is the acquisition cost of the 8 kWh Li-Ion battery, and it is set in 7500 €, L is the life time of the battery and Δt the time step. The end of life criterion is defined to be 80% of initial capacity C [27]. Therefore, the expected battery life can be calculated as $C = 0.8 = 1 - \psi L^{0.75}$, so the following equation remains:

$$K_t^{\text{calendar}}(V,T,\Delta t) = \frac{K^{\text{investment}}}{\frac{0.2}{((a \cdot V_t^{\text{cell}} - b) \cdot e^{-c/T})^{1/0.75}}} \Delta t \tag{9}$$

A linear approximation to (9) is calculated to relax the constraint and implement a linear solving method. Fig. 2 shows both nonlinear and linear equations, proving that the functions' behavior is practically identical.

Therefore, the linearized $K_t^{\text{cal,linear}}$ per time step t is formulated as

$$K_t^{\text{calendar,linear}}(V) = 0.019 \cdot V_t^{\text{cell}} - 0.0629 \tag{10}$$

2) Battery Constraints: The battery model constraints are formulated. The variable σ_t^{soc} in (11) represents the battery SOC for each period. To represent the real behavior of the battery, the efficiency factors for storing η^{ch} and delivering electricity η^{dis} are considered. The variables σ_t^{ch} and σ_t^{dis} represent the amount of energy charged or discharged in each period

$$\sigma_t^{\text{soc}} = \sigma_{t-1}^{\text{soc}} + \sigma_t^{ch} \cdot \eta^{ch} - \frac{\sigma_t^{\text{dis}}}{\eta^{\text{dis}}} \tag{11}$$

To avoid overoptimistic results, the battery SOC must be the same at the beginning and the end of the optimization horizon

$$\sigma_{t=0}^{\text{soc}} = \sigma_{t=\text{final}}^{\text{soc}} \tag{12}$$

As mentioned previously, it is essential to ensure that the battery is not fully charged or discharged by limiting its maximum and minimum allowed SOC to a specific fixed value to avoid cycle aging. Equation (13) ensures that σ_t^{soc} is always between a minimum $O^{\min}$ and a maximum $O^{\max}$ to preserve and extend the battery life time

$$O^{\min} \leq \sigma_t^{\text{soc}} \leq O^{\max} \tag{13}$$

Equations in (14) also help to minimize cycling aging by limiting the maximum power allowed for charging Q^{ch} and discharging Q^{dis}

$$\sigma_t^{ch} \leq \frac{Q^{ch}}{N^{\text{hour}}}, \qquad \sigma_t^{\text{dis}} \leq \frac{Q^{\text{dis}}}{N^{\text{hour}}} \tag{14}$$

Equations in (15) make sure that the energy charged per period σ_t^{ch} is linearly decreased. S^{ch} is the threshold in charging process. The same happens with the discharging energy σ_t^{dis}. The threshold to limit the energy output is S^{dis}

$$\sigma_t^{ch} \leq \frac{-Q^{ch}}{1 - S^{ch}} \left(\frac{\sigma_t^{\text{soc}}}{O^{\max}} - 1 \right), \quad \sigma_t^{\text{dis}} \leq \frac{Q^{\text{dis}}}{S^{\text{dis}}} \frac{\sigma_t^{\text{soc}}}{O^{\max}} \tag{15}$$

C. PV Generation Constraints

The formulation of a reducible PV generation model is presented. The optimization variable PV scheduled generation ψ_t^{pv} must be between 0 and the PV baseline electricity generation

TABLE IV
CASE STUDIES PARAMETERS

Parameters	Value	Units
Battery maximum allowed SOC	8	kWh
Battery minimum allowed SOC	2	kWh
Battery SOC initial/final	4.5	kWh
Battery maximum power charge/discharge	3	kW
Battery efficiency charge/discharge	0.95	-
Household maximum import capacity	6	kW
PV maximum output power	4.8	kW

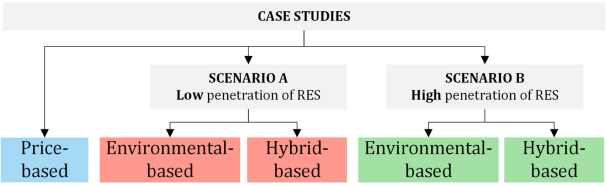

Fig. 3. Scheme of the case studies proposed to test HEMS programs performance.

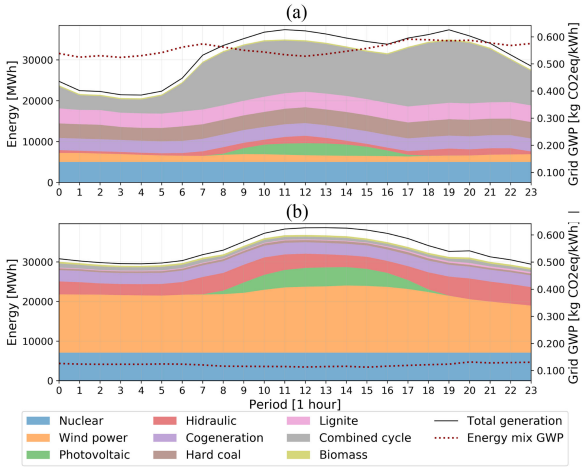

Fig. 4. Generation sources share considered for both scenarios. (a) Scenario A: low penetration of carbon free generation. (b) Scenario B: high penetration of carbon-free generation.

W_t^{pv}, which is the forecasted PV generation curve for the following day:

$$0 \leq \psi_t^{\text{pv}} \leq W_t^{\text{pv}} \tag{16}$$

IV. CASE STUDIES

The case studies presented in this section aim to analyze the three HEMS program's performance -PB, EB, and HB- to compare the electricity expenses and kg of CO_{2-eq} related to a single-family household. Real consumption and PV generation data are taken from the data port database [28] and used as input to the HEMS programs. These case studies are located in Spain; therefore, the Spanish dynamic electricity tariff (Precio Voluntario Pequeño Consumidor tariff) and its electricity mix are used as input data. P^{VAT} is set to 21%. The optimization horizon is 24 h, divided into 96 time periods of 15 min, starting at 00:00 h. The household contracted maximum power is 6 kW and is equipped with a 4.8 kW PV and an 9 kWh battery, whose SOC must be at least 50% at the beginning and end of the optimization horizon. The value of the parameters applied for all the case studies are listed in Table IV. The end-user does not sell back electricity to the grid; therefore, the PV is exclusively for self-consumption, and the excess of production can be stored in the battery for later usage. The HB multiobjective function weights are set to $\alpha = 0.3$ and $\beta = 0.7$, according to the end-user preferences that emphasize environmental aspects. The HEMS has been implemented in Python, using the Pyomo optimization library and the Gurobi solver. The optimal solution of the HB HEMS program was obtained with a computational time of 0.44 s on a Laptop with a processor core i7 at 2,60 GHz and 8 GB of RAM.

Two opposite scenarios of the Spanish energy mix generation are proposed to examine the HEMS program's performance. On the one hand, low penetration of renewables in the electricity mix and, on the other, high participation of sustainable generation sources. A scheme of these case studies is presented in Fig. 3. The PB HEMS is run separately since its performance only depends on the dynamic pricing tariff, regardless of the energy mix composition, since its objective is to minimize the cost, not GHG emissions. Case studies have identical inflexible demand, PV generation, battery parameters, and hourly electricity prices to compare the results of the three HEMS programs. The only input parameter that changes is the electricity generation mix of the grid.

For Scenario A with low RES penetration, data from November 20th 2017 is used, which percentage of nonfossil generation penetration is 29.18%. For Scenario B with high RES penetration, March 6th 2020 has been selected, with a daily average of 83.07% of electricity generation sources with zero emissions during their electrical grid operation. It should be noted that nuclear power is incorporated within the zero-emissions energy sources. The hourly share of each generation source—listed in Table II—in the Spanish energy mix for both scenarios is illustrated in Fig. 4. The total generation curve is also represented to demonstrate that the selected generation types are primarily responsible for the overall generation and cover 96% of the total demand. The higher the RES penetration in the energy mix is, the lower the GWP grid value per energy unit. Combined cycle and coal generation dominate in Fig. 4(a), while wind power does it in Fig. 4(b).

V. RESULTS

In this section, the case studies' results are presented and discussed. For a better understanding of the graphical outcomes obtained (see Fig. 5, for instance), it should be noted that negative energy values represent a generation source like PV and battery discharging. In contrast, positive values represent energy consumption, such as inflexible loads or battery charging. Therefore, due to the energy balance (2c), where generation must match consumption, the resulting plot is symmetrical if all the generation and consumption sources are summed up separately.

A. Price-Based Scenario

The PB case study analyzes the HEMS behavior under dynamic price tariff with the explicit aim of minimizing the

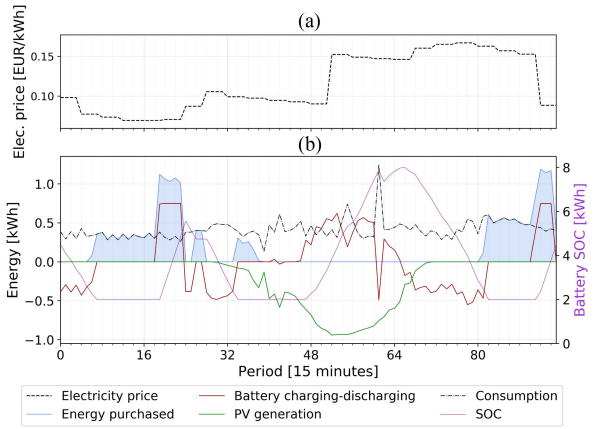

Fig. 5. Results of price-based HEMS under a Spanish price scheme. (a) Electricity price. (b) PB EMS.

end-user electricity cost. The PB objective function result is identical for high and low RES penetration scenarios since it only depends on the electricity tariff variation. However, the GHG emissions indirectly caused by PB optimization vary depending on the scenario. For clarification, the PB program is executed if the parameters are set to $\alpha = 1$ and $\beta = 0$ in the HB MOP, as (4a) indicates.

The PB HEMS optimization results are displayed in Fig. 5. The upper graph shows the electricity price, while the lower displays the PB optimization result. Focusing in Fig. 5(b), during periods of low prices (4–27), the consumed electricity is purchased directly from the grid, taking advantage as well to charge the battery (19–23, 91–94) to discharge it later during time intervals with more expensive costs (28–33, 66–81). PV allows self-consumption during most daylight periods, and the surplus energy is used to charge the batteries, reaching the maximum capacity of 8 kWh in period 66. The battery is charged again in the last low-priced periods (91–94) to meet the restriction of ending at least half of its SOC. The total cost of the objective function is 2.79 €. If the result is broken down, 52% belongs to battery degradation cost, while 48% corresponds to the price of buying electricity from the grid, including taxes.

B. Scenario A: Low Penetration of RES in the Energy Mix

The outcomes obtained in Scenario A for EB and HB HEMS programs are displayed in Fig. 6. The hourly-varying GWP of the grid along with electricity prices are represented in Fig. 6(a). Fig. 6(b) displays the EB and Fig. 6(c) shows the HB results.

The EB program is fed from the grid during periods with moderate kg CO_{2-eq} levels (0–27) compared to the daily GWP average. In periods of high grid GWP indicators, the battery is discharged (28–35) to avoid consuming from the network. PV generation is diminished (43, 46, 52, 54) as it is not possible to store the surplus energy in the battery due to its SOC limits. Besides, the sum of the kg of CO_{2-eq} per kWh of PV and the battery charge has a higher environmental impact than purchasing straight from the grid in specific periods. To comply with the battery SOC restriction at the end of the optimization horizon, electricity is bought from the grid to charge the battery when the grid GWP levels are low (see periods 38–60).

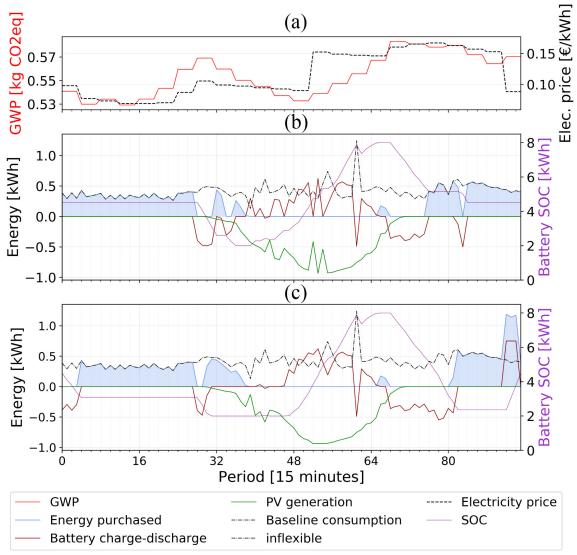

Fig. 6. Results of an environmental-based and hybrid-based HEMS in Scenario A under a Spanish price scheme. (a) Grid GWP and electricity price. (b) EB EMS. (c) HB EMS.

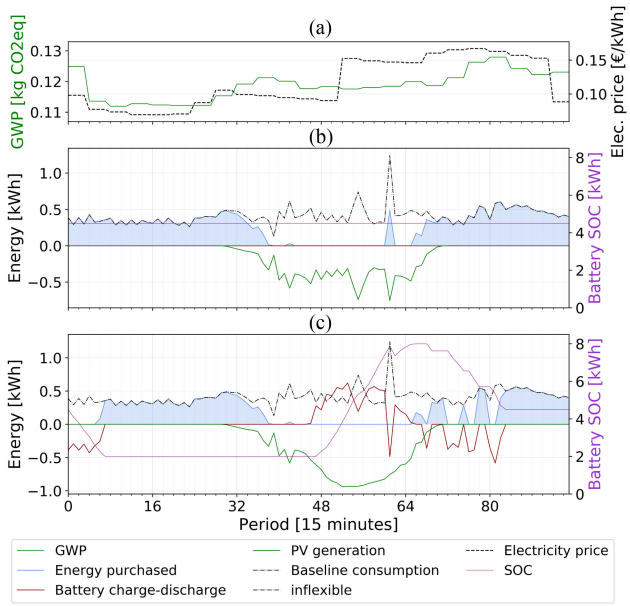

Fig. 7. Results of an environmental-based and hybrid-based HEMS in Scenario B under a Spanish price scheme. (a) Grid GWP and electricity price. (b) EB EMS. (c) HB EMS.

Concerning the HB HEMS program in Fig. 6(c), it is discerned that compared with the EB HEMS, the battery discharges at moderately high prices compared to the next periods (0–3). In (28–30), the battery discharges due to the high GWP values in the power system, although less energy than the EB, as the prices for that period are more high-priced. Solar energy does not reduce its production and is used for self-consumption. Meanwhile, the surplus energy is used for charging the battery. The HB avoids buying during the most expensive intervals of the day (76–80). The energy needed to charge the battery until the SOC imposed (4.5 kWh) at the end of the optimization horizon is purchased from the grid at affordable prices (91–96).

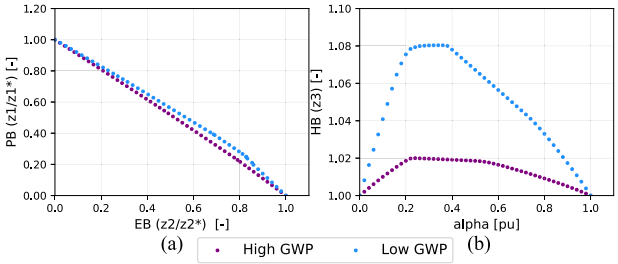

Fig. 8. (a) Pareto front and (b) HB solution values for high and low GWP scenarios.

C. Scenario B: High Penetration of RES in the Energy Mix

The electricity generation of the grid is composed of 83% on average by CO_2 free generation sources, including nuclear energy, and RES. Grid GWP values are 4.5 times lower than in the previous Scenario A, while the price signals, inflexible household consumption, and PV remain the same. EB HEMS results are shown in Fig. 7(b). Due to the high penetration of renewables in the electrical system, the EB purchases energy from the grid practically in its entirety, excluding daylight hours when the household is self-supplied, generating just the electricity required to meet the consumption. The EB program outcomes confirm that if a nation's energy mix is highly renewable as in Scenario B, the usage of batteries is more polluting than purchasing directly from the grid.

The HB HEMS outcomes are represented in Fig. 7(c). It avoids purchasing from the grid during expensive periods (0–6) and intermittent periods (68–82). It uses the PV surplus (46–65) to charge the battery and discharge it later during the high prices (68–72).

D. Sensitivity Analysis

The Pareto optimal front for the two HB normalized objective components are represented in Fig. 8(a), choosing as weighting factors α varying from 0 to 1 in steps of 0.02 and $\beta = 1 - \alpha$. The blue and purple points sequences represent the border of the feasible solution region that satisfies all the restrictions imposed for each GWP scenario. Fig. 8(b) shows the z_3 optimal solutions for each α for high and low GWP scenarios.

A sensitivity analysis is performed in Fig. 9 to show how the HB objective function z_3 is affected based on changes in the following input variables: maximum allowed battery SOC in Fig. 9(a) and (b), PV generation output in Fig. 9(c) and (d), inflexible household consumption in Fig. 9(e) and (f), and electricity price average in Fig. 9(g) and (h) for low and high GWP scenarios. The legend shows the maximum allowed SOC, the total daily PV generation and consumption, and the average daily electricity price. Thanks to this sensitivity study, it is known how the variation of one parameter affects the HB HEMS optimal solution, reducing uncertainty. It is reminded that $\alpha = 0$ corresponds to the EB HEMS program and $\alpha = 1$ to the PB HEMS program. The continuous gray line refers to the case study optimal solution described in Section IV and displayed in Fig. 8(b). The start and end of α take the value one due to the normalization of HB objective function z_3. Consumption is the variable that most affects the HB program. The lower

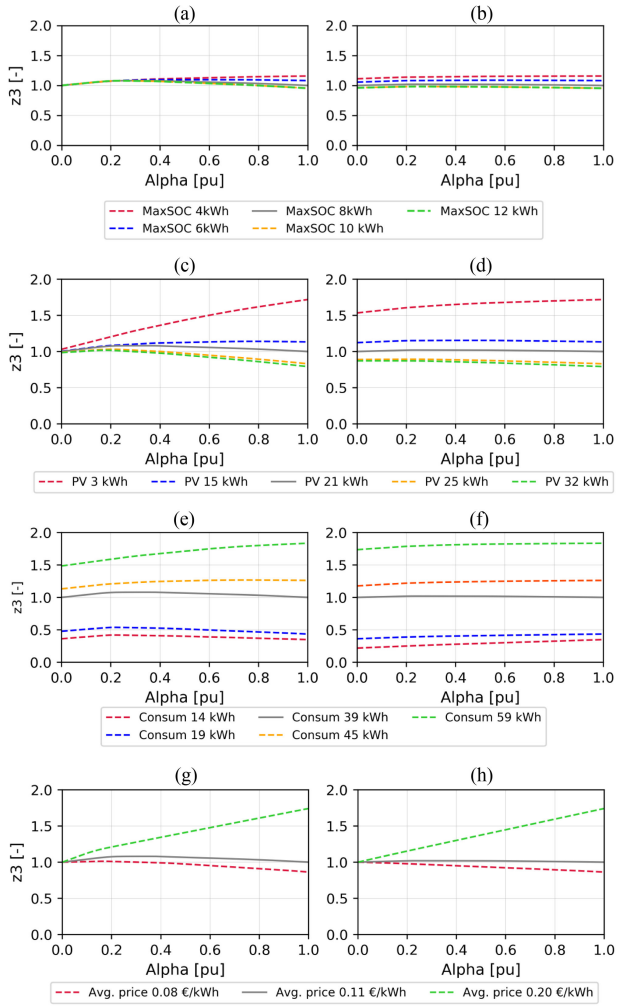

Fig. 9. Sensibility analysis of different HEMS input parameters. (a) Battery low GWP. (b) Battery high GWP. (c) PV low GWP. (d) PV high GWP. (e) Consumption low GWP. (f) Consumption high GWP. (g) Electricity price low GWP. (h) Electricity price high GWP.

the consumption, the lower the energy cost and emissions (see consum 14 kWh). On the contrary, the higher the consumption, the greater the cost and environmental impact (see 59 kWh). Consumption is followed by the electricity price, although when α equals to zero, this variable is insignificant since the EB HEMS does not consider the electricity price on its objective. The PV generation is more sensitive when it produces less (3 kWh) as this implies an increment in the electricity cost ($\alpha = 1$) because more electricity needs to be bought, but it has barely any impact for high amounts of generation (see PV 25 kWh and PV 32 kWh) because the household consumption is minimal compared with the PV generation. Finally, the input parameter that has the least influence is the maximum SOC allowed for the battery.

E. Results Comparison and Discussion

A comparative overview of the HEMS program results for both high and low RES penetration scenarios is presented in Table V, where the total GHG emissions and electricity costs are shown. Moreover, these HEMS programs are compared with the household baseline, which is the energy exchanged with the grid if no flexible resources were activated. In other words, the

TABLE V
RESULTS OF THE CASE STUDY $\alpha = 0.3$ $\beta = 0.7$ GHG EMISSION AND ENERGY COSTS COMPARISON BETWEEN THE DIFFERENT ENERGY MANAGEMENT SYSTEM PROGRAMS

HEMS program	GHG [kg CO_{2-eq}]		Electricity cost [€]	
	High RES	Low RES	High RES	Low RES
Price-based program	5.33	14.39	1.33	1.33
Hybrid-based program	4.85	13.96	2.74	2.54
Environmental-based program	4.62	13.68	3.74	2.70
Baseline consumption	4.72	22.08	5.73	5.73

end-user buys all the power from the grid to meet the inflexible consumption. It is concluded that PB HEMS achieves the lowest electricity costs for both scenarios as expected, due to avoiding the purchase from the grid during expensive periods. However, in return, the PB HEMS has the most polluting emissions associated with its consumption, specifically releases 15.36% more emissions than the less polluting program—the EB—in the high RES scenario. On the other hand, the PB produces 5.19% more emissions than the EB in the low RES scenario. On the economic side, the EB program pays 2.81 times more in the electricity bill than the PB in high RES situation and almost twice as much in a low RES scenario.

As can be appreciated in Table V, the HB program has a balance between the PB and EB programs. For high presence of renewables in the energy mix, the difference between the HEMSs emissions does not exceed a range of 15%, while in the opposite RES scenario, the boundary is narrowed to approximately 5%. This is because during periods of high renewable generation in the energy mix, the EB purchases from the grid most of the periods, so the battery is not utilized for self-supply, neither is charged by PV surplus, resulting in a higher electricity bill when buying more energy from the grid.

The baseline case only emits 2% more pollutant emissions than the EB program in the high RES scenario. The explanation is the same as in the previous paragraph: energy from the grid is cleaner than discharging batteries previously charged with solar PV surplus. On the contrary, on days with a high percentage of fossil-type generation in the grid, the kg of CO_{2-eq} soared compared to the rest of the programs: 61% more emissions than EB, 58.16% compared to HB, and 53.44% compared to PB. The explanation is that the rest of the HEMS programs use the surplus PV generation to charge batteries for later use, avoiding to a great extent buying from the grid, which is much more polluting than the use of flexible resources.

VI. CONCLUSION

This article introduces a novel hybrid-based HEMS formulation that optimizes the operation of PV generators and distributed storage units behind-the-meter in order to achieve the best trade-off between electricity cost and GHG emissions minimization, considering a life cycle analysis of the generation sources used to meet the household demand. Two facing energy mix scenarios are proposed: high renewable energy participation and high fossil-type generation participation. The results confirm the reduction of GHG emissions in the HEMS containing the environmental component. The EB program achieves the lowest emissions, while the HB seeks a compromise between economic and environmental factors. By assigning weights to the HB multiobjective function, the end-user can modify its priority in a fast and flexible manner.

The more renewable generation is in the energy mix, the lesser the difference between the HEMS programs' emissions and the baseline case. However, electricity costs increase the more renewable energy is in the energy mix. Therefore, if the objective is strictly to minimize the environmental impact produced by the household consumption, it is concluded that if a nation regularly holds a very high penetration of renewable generation in its energy mix as it occurs in Scenario B, it is more sustainable from the household point of view to buy electricity directly from the grid than using self-consumption with batteries, previously charged with PV surplus, for instance. In return for prioritizing and considering the polluting emissions minimization, the HB HEMS electricity expenses can be two times higher than the PB. On the other hand, for countries with low penetration of renewable generation sources in the energy mix, flexible resources such as batteries and PV panels significantly reduce GHG emissions and costs. Therefore, HB HEMS is an excellent option to encourage end-users to participate in the fight against climate change without causing high economic expenses. It should be noted that, if second-life batteries were used for this purpose in the future, the value of the GWP parameter would be reduced, and the conclusions obtained in this article could vary. Finally, the sensitivity analysis carried out for a set of input variables indicates that household consumption is the input variable that most affects the HB objective function's results, followed by PV generation, electricity price, and maximum allowed SOC, respectively.

ACKNOWLEDGMENT

The authors would like to thank Pecan Street Inc. Dataport database for providing real household data.

REFERENCES

[1] International Energy Agency, "Global CO2 emissions in 2019 – analysis," Accessed: Sep. 2020. [Online]. Available: https://www.iea.org/articles/global-co2-emissions-in-2019

[2] DNV GL's, "Energy transition outlook 2019 - A global and regional forecast to 2050," DNV GL's Group Technology & Research, 2019, pp. 1–290, 2019, doi: 10.2307/j.ctv7xbrmk.21.

[3] IEA, IEA, "Perspectives for the clean energy transition- the critical role of buildings," International Energy Agency, pp. 1–114, Apr. 2019. [Online]. Available: https://webstore.iea.org/perspectives-for-the-clean-energy-transition

[4] Y. Kwon, T. Kim, K. Baek, and J. Kim, "Multi-objective optimization of home appliances and electric vehicle considering customer's benefits and offsite shared photovoltaic curtailment," *Energies*, vol. 13, no. 11, 2020, Art. no. 2852.

[5] M. Jaclason *et al.*, "A multi-objective demand response optimization model for scheduling loads in a home energy management system," *Sensors*, vol. 18, no. 10, 2018, Art. no. 3207.

[6] R. Reghukumar, S. Sambhu, and V. Ravikumar Pandi, "Multi-objective optimization for efficient home energy management system using differential evolution algorithm," in *Proc. 3rd IEEE Int. Conf. Recent Trends Electron., Inf. Commun. Technol.*, 2018, pp. 1157–1162.

[7] X. Wang, X. Mao, and H. Khodaei, "A multi-objective home energy management system based on internet of things and optimization algorithms," *J. Building Eng.*, vol. 33, 2021, Art. no. 101603.

[8] M. C. Di Piazza, G. La Tona, M. Luna, and A. Di Piazza, "A two-stage energy management system for smart buildings reducing the impact of demand uncertainty," *Energy Buildings*, vol. 139, pp. 1–9, 2017.

[9] G. Huang, J. Yang, and C. Wei, "Cost-effective and comfort-aware electricity scheduling for home energy management system," in *Proc. IEEE Int. Conf. Big Data Cloud Comput.*, 2016, pp. 453–460.

[10] K. Dittawit and F. A. Aagesen, "Home energy management system for electricity cost savings and comfort preservation," *Proc. IEEE Int. Conf. Consum. Electron.*, 2015, pp. 309–313.
[11] N. Javaid *et al.*, "Towards cost and comfort based hybrid optimization for residential load scheduling in a smart grid," *Energies*, vol. 10, no. 10, pp. 1–27, 2017.
[12] M. Waseem, Z. Lin, S. Liu, A. Intisar Sajjad, and T. Aziz, "Optimal GWCSO-based home appliances scheduling for demand response considering end-users comfort," *Elect. Power Syst. Res.*, vol. 187, 2020, Art. no. 106477.
[13] T. Sattarpour, D. Nazarpour, and S. Golshannavaz, "A multi-objective HEM strategy for smart home energy scheduling: A collaborative approach to support microgrid operation," *Sustain. Cities Soc.*, vol. 37, pp. 26–33, 2018.
[14] M. A. F. Ghazvini, João Soares, O. Abrishambaf, R. Castro, and Z. Vale, "Demand response implementation in smart households," *Energy Buildings*, vol. 143, pp. 129–148, 2017.
[15] S. Barja-Martinez, I. Munne-Collado, P. Lloret-Gallego, M. Araques-Penalba, and R. Villafafila-Robles, "A novel home energy management system environmental-based with LCA minimization," in *Proc. IEEE Int. Conf. Environ. Elect. Eng.*, Madrid, Spain, 2020, pp. 1–6.
[16] T. Xing, H. Lin, Z. Tan, and L. Ju, "Coordinated energy management for micro energy systems considering carbon emissions using multi-objective optimization," *Energies*, vol. 12, no. 23, 2019, Art. no. 4414.
[17] A. Mahmood *et al.*, "An enhanced system architecture for optimized demand side management in smart grid," *Appl. Sci.*, vol. 6, no. 5, 2016, Art. no. 122.
[18] X. Jin, K. Baker, D. Christensen, and S. Isley, "Foresee: A user-centric home energy management system for energy efficiency and demand response," *Appl. Energy*, vol. 205, pp. 1583–1595, 2017.
[19] M. Shakeri *et al.*, "An intelligent system architecture in home energy management systems (HEMS) for efficient demand response in smart grid," *Energy Buildings*, vol. 138, pp. 154–164, 2017.
[20] T. HieuNguyen, T. DuongNguyen, and Long B. Le, "Energy management for households with solar assisted thermal load considering renewable energy and price uncertainty," *IEEE Trans. Smart Grid*, vol. 6, no. 1, pp. 301–314, Jan. 2015.
[21] F. Wang *et al.*, "Smart households' aggregated capacity forecasting for load aggregators under incentive-based demand response programs," *IEEE Trans. Ind. Appl.*, vol. 56, no. 2, pp. 1086–1097, Mar./Apr. 2020.
[22] M. Luisa DI Silvestre, P. Gallo, E. R. Sanseverino, G. Sciume, and G. Zizzo, "Aggregation and remuneration in demand response with a blockchain-based framework," *IEEE Trans. Ind. Appl.*, vol. 56, no. 4, pp. 4248–4257, Jul./Aug. 2020.
[23] R. Turconi, A. Boldrin, and T. Astrup, "Life cycle assessment (LCA) of electricity generation technologies: Overview, comparability and limitations," *Renewable Sustain. Energy Rev.*, vol. 28, pp. 555–565, 2013.
[24] I. Munné-Collado, Fabio Maria Aprà, P. Olivella-Rosell, and R. Villafáfila-Robles, "The potential role of flexibility during peak hours on greenhouse gas emissions: A life cycle assessment of five targeted national electricity grid mixes," *Energies*, vol. 12, no. 23, 2019, Art. no. 4443.
[25] E. Redondo-Iglesias, P. Venet, and S. Pelissier, "Modelling lithium-ion battery ageing in electric vehicle applications-calendar and cycling ageing combination effects," *Batteries*, vol. 6, no. 1, pp. 1–18, 2020.
[26] J. Schmalstieg, S. Käbitz, M. Ecker, and D. U. Sauer, "A holistic aging model for Li(NiMnCo)O2 based 18650 lithium-ion batteries," *J. Power Sources*, vol. 257, pp. 325–334, 2014.
[27] F. Rücker, I. Bremer, S. Linden, J. Badeda, and D. U. Sauer, "Development and evaluation of a battery lifetime extending charging algorithm for an electric vehicle fleet," *Energy Procedia*, vol. 99, pp. 285–291, 2016.
[28] Pecan Street Inc. Dataport Database, 2020. [Online]. Available: https://www.pecanstreet.org/dataport/

Sara Barja-Martinez received the M.Sc. degree in industrial engineering (major in energy) from the Universitat Politëcnica de Catalunya (UPC), Barcelona, Spain, in 2018. She is currently working toward the doctoral degree in electrical engineering from CITCEA-UPC, Barcelona, Spain, focusing on power system flexibility, optimization, and machine learning techniques at the distribution grid level.

Since 2017, she has been working on several innovative projects with the CITCEA-UPC research group. Her research interests include energy management system algorithms, machine learning techniques applied to the energy field, electricity and flexibility markets, optimization, and demand response programs.

Fabian Rücker received the M.Sc. degree in physics from the Ludwig-Maximilians-Universität München, Munich, Germany, in 2013 . He is currently working toward the doctoral degree in electrical engineering with RWTH Aachen University, Aachen, Germany, in the field of grid integration of electric vehicles and storage systems.

He is an Engineer with CITCEA-UPC, and the Department of Electrical Engineering, Universitat Politëcnica de Catalunya, Barcelona.

Mònica Aragüés-Peñalba received the M.Sc. degree in industrial engineering (major in electricity) and the Ph.D. degree in electrical engineering from the School of Industrial Engineering of Barcelona, Universitat Politècnica de Catalunya (UPC), Barcelona, Spain, in 2011 and 2016, respectively.

Since 2010, she has been with CITCEA-UPC, and with the Departmnt of Electrical Engineering, UPC. Since April 2018, she has been a Lecturer with the Department of Electrical Engineering, UPC (Serra Hunter Fellow). She is currently the Project Co-ordinator of BD4OPEM H2020. Her research interests include renewable integration in power systems, transmission and distribution power systems, wind and solar power plants operation and control, microgrids operation and control, optimization, and data science applications to power systems.

Roberto Villafafila-Robles received the M.Sc. degree in industrial engineering and the Ph.D. degree in electrical engineering from the School of Industrial Engineering of Barcelona, Universitat Politècnica de Catalunya (UPC), in 2005 and 2009, respectively.

He is currently an Associate Professor with the Department of Electrical Engineering, UPC. Since 2003, he has been with the CITCEA-UPC, where he is involved in technology transfer with the local industry due to research and innovation. His research interests include integration of renewable energy–storage–electrical vehicles into power systems, electricity markets, and energy and territory

Íngrid Munné-Collado received the M.Sc. degree in industrial engineering from the School of Industrial Engineering of Barcelona, Universitat Politècnica de Catalunya (UPC), in 2015, where she is currently working toward the Ph.D. degree in electrical engineering.

Since 2015, she has been with the CITCEA-UPC research group. Her research interests include local electricity markets, life-cycle assessment, innovation on higher education, demand-response, optimization in power systems, and flexibility services for aggregators and DSOs.

Pau Lloret-Gallego received the M.Sc degree in industrial engineering from the School of Industrial Engineering of Barcelona, Universitat Politècnica de Catalunya (UPC), in 2006.

In 2004, he was the CITCEA-UPC staff, where he is currently Senior Project Manager developing innovation projects for the power system industry. His research interests include power system engineering, distribution automation and communications, energy markets, and distributed generation.